

HOSTED BY



Contents lists available at ScienceDirect

Saudi Pharmaceutical Journal

journal homepage: [www.sciencedirect.com](http://www.sciencedirect.com)

Original article

# Microsponge-derived mini tablets loaded with immunosuppressive agents: Pharmacokinetic investigation in human volunteers, cell viability and IVIVC correlation



Yasir Mehmood <sup>a,\*</sup>, Hira Shahid <sup>b</sup>, Muhammad Abbas <sup>c</sup>, Umar Farooq <sup>d</sup>, Shaukat Ali <sup>e</sup>, Mohsin Kazi <sup>f,\*</sup>

<sup>a</sup> Riphah Institute of Pharmaceutical Sciences (RIPS), Riphah International University, Faisalabad, P. O. Box 38000, Pakistan

<sup>b</sup> Department of Pharmacology, Faculty of Pharmaceutical Sciences, Government College University Faisalabad, P.O. Box 38000, Pakistan

<sup>c</sup> Imran Idress College of Pharmacy, Sialkot P.O. Box 51310, Pakistan

<sup>d</sup> Faculty of Pharmacy, Grand Asian University, Sialkot, Punjab P.O. Box 51310, Pakistan

<sup>e</sup> Ascendia Pharma, Inc. North Brunswick, NJ 08902 USA

<sup>f</sup> Department of Pharmaceutics, College of Pharmacy, P.O. Box 2457, King Saud University, Riyadh 11451, Saudi Arabia

## ARTICLE INFO

### Article history:

Received 13 February 2023

Accepted 20 September 2023

Available online 26 September 2023

### Keywords:

Sirolimus  
Solubility  
Solid dispersions  
Bioavailability  
IVIVC

## ABSTRACT

Sirolimus, a potent immunosuppressant, has been demonstrated to have remarkable activity in inhibiting allograft rejection in transplantation. The objective of the study was to fabricate microsponge mini tablets with enhanced solubility and bioavailability.  $\beta$ -Cyclodextrin and NEOCEL C91 were selected to prepare the microsponges (SLM-M) to improve the stability and solubility of sirolimus. The current study involved the quasi emulsion-solvent diffusion technique to design sirolimus-loaded microsponges that were further compressed into mini tablets 4 mm in diameter. Solid-state characterization, dissolution at different pH values, stability, and pharmacokinetic profiles with IVIVC data were analyzed in humans. Fourier transform infrared (FTIR) spectroscopy, differential scanning calorimetry (DSC), and X-ray diffraction (XRD) were used to characterize the formulations, and high-performance liquid chromatography (HPLC) was used to assess the drug stability of the compressed microsponge minitables. The API changed from the crystalline state to an amorphous state, as shown by XRD and DSC. The compressed mini tablets showed a 4-fold enhancement in the drug dissolution profile. A toxicology investigation suggested that mini tablets were safe. In humans, the bioavailability of sirolimus compressed mini tablets from SLM-M was significantly improved. The results suggest that mini tablets prepared with  $\beta$ -cyclodextrin and NEOCEL C91 by a quasi emulsion-solvent diffusion process might be an alternative way to improve the bioavailability of sirolimus. In addition, the manufacturing process is easily scalable for the commercialization of drugs to market.

© 2023 The Author(s). Published by Elsevier B.V. on behalf of King Saud University. This is an open access article under the CC BY-NC-ND license (<http://creativecommons.org/licenses/by-nc-nd/4.0/>).

## 1. Introduction

Several strategies have been employed in recent decades to enhance the aqueous solubility and effective administration of water-insoluble drugs (Bansal et al. 2011). The method to prepare

$\beta$ -cyclodextrin and NEOCEL C91 microsponges requires a quasi emulsion-solvent diffusion technique, which is a novel method applied in the field of pharmaceutical technology (Muëller et al. 2000). This method adopts a simple manufacturing procedure and has the advantages of controlling drug release by diffusion (Muëller et al. 2000). Optimization of the formulation is necessary for the efficient design of drug release from the dosage form (Huang et al. 2004). The polymers used are synthetic and natural. Polymers are naturally occurring polysaccharides that are extracted from plants and have been used in several pharmaceutical products (Beneke et al. 2009; Deshmukh and Aminabhavi 2015). The main sources of these natural polymers are rain-fed and irrigated agricultural cultivation that can produce polysaccharides (Zaharuddin et al. 2014). Polysaccharides are from renewable sources, stable, and widely available, and hence, they are often

\* Corresponding authors.

E-mail addresses: [Yasir\\_dpharm@hotmail.com](mailto:Yasir_dpharm@hotmail.com) (Y. Mehmood), [shaukat.ali@ascendiaipharma.com](mailto:shaukat.ali@ascendiaipharma.com) (S. Ali), [mkazi@ksu.edu.sa](mailto:mkazi@ksu.edu.sa) (M. Kazi).

Peer review under responsibility of King Saud University.



Production and hosting by Elsevier

<https://doi.org/10.1016/j.jsps.2023.101799>

1319-0164/© 2023 The Author(s). Published by Elsevier B.V. on behalf of King Saud University.

This is an open access article under the CC BY-NC-ND license (<http://creativecommons.org/licenses/by-nc-nd/4.0/>).

used as raw materials (Crini 2005; Aboulrous et al. 2016). There are some disadvantages of natural polymers, however, as they are used in larger quantities to achieve the desired results. Furthermore, these natural polymers tend to swell and control drug release. Among the semisynthetic polymers are naturally occurring cyclic oligosaccharides, which are water soluble and composed of  $\alpha$ -1,4-linked D-glucopyranose units known as cyclodextrins (CDs). Due to their high molecular weight, high water solubility and low toxicity, their use in pharmaceuticals is very common (Yuvaraja and Khanam 2014).

Sirolimus is a naturally occurring macrolide antibiotic and is insoluble in water. It is synthesized by the bacterium *Streptomyces hygroscopicus*. It acts by selectively blocking the transcriptional activation of cytokines, resulting in inhibition of cytokine synthesis pathways (Preetham and Satish 2011). Upon binding to immunophospholipins, it becomes bioactive. It is a potent immunosuppressant that is used in preventing kidney and liver transplant rejections (Rangan et al. 2009). It is also used for the treatment of psoriasis and dermatitis (Ormerod et al. 2005). Antifungal and antineoplastic effects are also two major therapeutic benefits of sirolimus. Thus, sirolimus possesses many therapeutic benefits and has potential for marketing against many life-threatening diseases. It has an aqueous solubility of 2.6  $\mu\text{g/ml}$  and a high molecular weight of 914 Da and possesses no functional group that is capable of ionizing between pH 1 and pH 10 (Shen and Wu 2007). Sirolimus has limited aqueous solubility and poor dissolution and absorption, hence leading to poor bioavailability (Shen et al. 2018). Following oral administration, sirolimus has absorbed in a dose-dependent fashion and attains the maximum blood concentration ( $C_{\text{max}}$ ) in an hour. In human transplant recipients, sirolimus has an oral bioavailability of approximately 15%. Extensive intestinal and hepatic first-pass metabolism of sirolimus by the cytochrome P4503A4 isoenzyme coupled with countertransport by multidrug efflux pump and intestinal P-glycoprotein result in large inter and inpatient variability in oral absorption. Therefore, it is important to formulate sirolimus mini tablets with micro-sponge novel technology to overcome its poor aqueous solubility and bioavailability challenges (Shen et al. 2018). There are studies reported in the literature on improving the solubility and bioavailability of sirolimus by using different technologies, but none is applicable for easy scale-up and commercialization. In our studies, we used a nonconventional method and selected less expensive and easily available excipients for the preparation of micro-sponge-based minitabets by using a quasiemulsion-solvent method that meets the regulatory guidelines. We observed that quasi emulsion-solvent diffusion is an efficient method for enhancing the solubility bioavailability of BCS II and IV drugs. The process is simple and requires technical skills and operational excellence for the successful development of formulations. We demonstrate that by employing this method, we can develop microsponges that can be compressed into mini tablets with commercially viable and easily available commonly used excipients. SEM (scanning electron microscopy), FT-IR (Fourier transform infrared spectroscopy), XRD (X-ray diffraction), and in vitro dissolution were used to determine the stability, structure, and release performance of compressed micro-sponge minitabets. Additionally, the parameters of mini tablets, including their friability, mean weight, and hardness, were assessed according to USP 43. Stability was also determined over 45 days under accelerated conditions at 45 °C/75% RH.

## 2. Materials and methods

### 2.1. Chemicals

Sirolimus (SLM) was gifted by Ameer & Adnan Pharmaceuticals (Lahore, Pakistan). Similarly, sodium hydrogen phosphate and

ethanol 99% were obtained from Merck KGA (Germany); acetone, acetonitrile, tween 60, dichloromethane, sodium dodecyl sulfate and phosphoric acid were obtained from Dae-Jung Chemicals Korea (analytical grade); colloidal microcrystalline cellulose with croscarmellose sodium (NEOCEL C91) was obtained from JRS (Germany); and  $\beta$ -cyclodextrin was obtained from AG (Darmstadt, Germany). All the reagents were of analytical grade and were used as received (see Table 1).

### 2.2. Preparation of microsponges using polymer

In the current research work, we used a quasiemulsion-solvent diffusion technique for the formulation of microsponges. In the organic phase, matrix-forming polymers such as  $\beta$ -cyclodextrin and NEOCEL C91 were dissolved in a 1:1 ratio (5.0 mL ethanol was used as solvent), and 0.50 mg of SLM in dichloromethane was dissolved and mixed with the ingredients in ethanol until a homogeneous dispersion medium was achieved. Five milliliters of Tween 60 in 100 mL of distilled water was added with continuous mixing by using a high-speed homogenizer (500 rpm). After 15 min of mixing, precipitation starts. As the ethanol was evaporated, porous microsponges (SLM-M) were produced, which were filtered with a 0.45- $\mu\text{m}$  size (Whatman) and dried at room temperature for 24 h. The dried powders were compressed into minitabets with other ingredients. Each mini tablet weighing 60.5 mg comprised 20 mg SLM-M (1 mg drug), 20 mg Avicel, 0.5 mg Mg Stearate, and 20 mg lactose. Tablets compression pressure was maintained 20–40 Mpa as it is low pressure to avoid microsponges breaking. The hardness of tablets was kept constant at 2–4 kg/cm<sup>2</sup>.

### 2.3. Percentage yield determination

Microsponge weight was recorded, and yield was calculated by comparing fabricated microsponges against the weight of cumulative polymer and drug (Mohammadpour Dounighi et al. 2016).

$$(\%) \text{ yield} = \frac{\text{mass of Microsponges obtained}}{\text{total mass of drug and polymer used}} \times 100$$

### 2.4. Determination of drug content

Drug in microsponges (SLM-M) was determined by dissolving in acetonitrile. The solvent was filtered by Millipore® filters with a pore size of 0.45  $\mu\text{m}$ . The solvent was collected and diluted further with the mobile phase to determine the drug by HPLC LC20A (Shimadzu) at  $\lambda_{\text{max}}$  250 nm. A standard calibration curve was constructed to determine the sirolimus concentrations.

### 2.5. Rheological studies of SLM-M

#### 2.5.1. Bulk density

Microsponges (SLM-M) were placed in a 10 mL measuring cylinder. The cylinder's initial volume was measured before it was permitted to tap on a hard, flat surface. After tapping, the

**Table 1**  
Optimized formulation of microsponges.

No.	Material Name	Quantity of Material Used
	Sirolimus	0.50 mg
	$\beta$ -cyclodextrin	200 mg
	NEOCEL C19	200 mg
	Ethanol	5 mL
	Dichloromethane	5 mL
	Tween 80	5 mL
	Water	100 mL

cylinder's volume was measured. Until there was no change in the volume, the process of tapping on a firm, flat surface was performed again. The following equations were used to calculate the solid dispersion's bulk density (BD) and tapped density (TD) (Montiel-Herrera et al. 2015).

$$BD = \frac{\text{weight of SLM} - M}{\text{volume of packing}}$$

$$TD = \frac{\text{weight of SLM} - M}{\text{tapped volume of packing}}$$

### 2.5.2. Carr's index or compressibility index

Carr's index is commonly used for the indirect measurement of rheological properties of materials. The following equation can be used for this purpose.

$$\text{Carr's index} = \frac{\text{initial volume} - \text{final volume}}{\text{initial volume}} \times 100$$

$C_i$  (Carr's index.) is used to represent the flow properties of the materials.

If  $C_i$  is <15%, the powder shows good flowability, while  $C_i$  greater than 25% shows poor flowability.

### 2.5.3. Hausner ratio

Hausner's ratio is used to determine the flow characteristics. The following equation is used for the determination of Hausner's ratio.

$$\text{Hausner's ratio} = \frac{\text{volume before tapping}}{\text{volume after tapping}}$$

### 2.5.4. Angle of repose

A funnel was taken, and microsponges (SLM-M) were poured into it. The loaded funnel was then poured on the horizontal surface. The angle of repose was calculated by determining the angle between the horizontal surface and height of the heap. The following equation is employed to determine the angle of repose.

$$\tan \theta = \frac{h}{r}$$

In the equation above, h shows the height of the pile, while r is the radius of the pile base.

## 2.6. Experimental development method for HPLC

The structure of sirolimus consists of a conjugated group and benzene ring; thus, it is a UV-active compound. Its maximum and specific absorbance ( $A = 1\%$ ), are both shown at  $\lambda_{\text{max}} = 250 \pm 1$ . The absorbance of the separate solution and composite reference solution containing SLM-M  $10 \mu\text{g/mL}$  was measured from 200 to 400 nm to obtain the optimal wavelength for concurrent identification at the sole wavelength of the UV detector. An environment framework (keeping in view the solubility and nature of each analyte) was laid down for greater resolution of both analytes by systematic elution of different mobile phases while maintaining different flow rates and diverse stationary phases. HPLC analysis was carried out on an LC-20AB (Shimadzu, Japan) with an attached UV-VIS detector (Shimadzu, Japan) and a column oven. An Agilent C18 Agela column (125 mm X 4.6 mm, 5  $\mu\text{m}$ ) was selected as the analytical column, and Chromtek software (version 5.3, Alltech, USA) was used to process the chromatographic data.

Reference solutions were prepared by isocratic elution of the mobile phase with diverse ratios of mobile phase over various columns, i.e., octyl silica (Si-[CH<sub>2</sub>]-CH<sub>3</sub>) C18. For the analyte, more appropriate resolution and symmetrical peaks were obtained in

the aggregate of acetonitrile and phosphoric acid (400:600), and the flow rate was maintained at 1 mL/min over 125 mm  $\times$  4.6 mm, 5  $\mu\text{m}$  C18. Chromatographic conditions were followed according to USP and ICH guidelines. USP < 1225 > Validation of Compensial Methods was used for the validation of the HPLC analytical method. The same process was used for the determination of SLM-M in human plasma according to the method described in the literature (M. Aqil 2007). A C18 column was used with acetonitrile and phosphoric acid (400:600) as the mobile phase and tacrolimus monohydrate as the internal standard (IS). The procedure is sensitive with a defined limit of quantification of 20 ng/mL. The calibration plot for SLM-M in plasma was linear in the concentration range of 20–200 ng/mL. The procedure can efficiently be applied for the analysis of SLM-M during pharmacokinetic studies in human plasma.

## 2.7. Transform infrared spectroscopy (FT-IR)

FT-IR analysis of the raw SLM, SLM-M and polymers was performed. Spectra were recorded using a Vertex 70 FT-IR spectrometer (Bruker, Billerica, MA, USA) with a resolution of 2  $\text{cm}^{-1}$  at room temperature. The range of the wavenumber was 4000–500  $\text{cm}^{-1}$  (Preetham and Satish 2011).

## 2.8. Scanning electron microscopy (SEM)

The surface morphologies of the neat SLM, polymers and microsponges (SLM-M) were determined by a Hitachi S-6000 scanning electron microscope (Preetham and Satish 2011).

## 2.9. Thermal analysis

TA Instruments' DSC-2010 (USA) differential scanning calorimeter was used to examine the thermal properties of sirolimus powder, polymers and microsponges (SLM-M). Samples weighing approximately 2 mg were placed on sealed aluminum pans, heated under a nitrogen flow rate of 25 mL/minute, and scanned at a rate of 10  $^{\circ}\text{C}/\text{min}$ . The temperature was kept constant in the range of 0 to 250 $^{\circ}\text{C}$  (Haeri et al. 2017).

## 2.10. Powder X-ray diffraction (PXRD)

By using an X-ray diffractometer (X'pert PRO-PAN analytical, Netherlands), powder X-ray diffractograms of pure drug, polymer and microsponges (SLM-M) were obtained. The device had a CuK radiation source and was running at 30 mA and 30 kV. Peak patterns were obtained with steps of 0.02 $^{\circ}$  at 2 angles ranging from 5 $^{\circ}$  to 50 $^{\circ}$ . A 4 $^{\circ}/\text{min}$  adjustment was made to the scanning speed (Shen et al. 2018).

## 2.11. In-vitro dissolution study of SLM-M

Utilizing USP apparatus II (Pharma Test, China), the in vitro dissolution test was assessed (Shazly and Mohsin 2015). After calculating the number of spins the paddle makes per minute, the apparatus was approved. 900 mL of 0.1 N hydrochloric acid and 900 mL phosphate buffer pH 7.4 were used for the dissolution tests at pH values of 1.2 and 7.4. The temperature and stirring speed were held at 37.0  $\pm$  0.5  $^{\circ}\text{C}$  and 50 rpm, respectively. Ten milliliter samples were taken at intervals of 5, 15, 40, 60, 80, and 120 min. Using HPLC, the amount of API in microspoon (SLM-M) mini tablets was determined at a wavelength of 250 nm. For comparison as a reference, sirolimus at pH 7.4 phosphate buffer and at pH 1.2 were used separately and run for approximately 120 min under similar HPLC conditions.

## 2.12. In vitro cell viability studies

The human hepatocellular (HepG2) cell line was obtained from the University of Lahore and made by American Type Culture Collection (ATCC) Manassas. Cells were grown to their full potential in DMEM supplemented with 10% (v/v) FBS in a humidified environment of 95% (v/v) and 5% (v/v) CO<sub>2</sub> at room temperature. Cells were seeded near confluence with SD-SLM the day before incubation. The MTT (3-(4,5-dimethylthiazol-2-yl)-2,5-diphenyltetrazolium bromide) test was used to quantify succinate dehydrogenase mitochondrial activity as an indicator of cell viability/proliferation. (Mosmann 1983). Different concentrations of SLM-M (50, 100, 200 and 400 µg/mL) were added to the cell medium for 24 h. Then, 15 µL of MTT (5 mg/mL) in phosphate buffered saline (PBS) was added to each well. It was incubated at 37 °C for an additional 4 h. The medium with MTT was then aspirated carefully. The formed formazan crystals in each well were solubilized in 100 µL of dimethyl sulfoxide (DMSO). A microplate reader was used for the determination of dissolved formazan crystals at 570 nm (Patel et al. 2009). The following equation was used to determine the percentage cell viability.

$$\% \text{cell Viability} = \frac{\text{Absoftreatedcell} - \text{Absofblank}}{\text{Absofcontrol} - \text{Absofblank}} \times 100$$

## 2.13. In- vivo studies

Pharmacokinetic (*in- vivo*) studies were performed for pure SLM and SLM-M in humans. Tabular and graphical forms were used to represent the plasma profile of the drug level. Pharmacokinetic analyses of the neat SLM and prepared SLM-M min tablets were carried out by adopting an observational, cross-sectional study design. Twelve patients who were already taking this medicine after transplantation were selected. A consent form was completed by all volunteers, and permission was granted by Rashid Latif Medical College and Pharmacy College. All males were selected for this study. A mean age of 54.3 ± 2.0 years and a mean body mass index (BMI) of 28.8 ± 1.5 kg/m<sup>2</sup> were enrolled in this study. According to their medical histories, a physical exam, and standard laboratory tests, all subjects were in good condition. For at least a week prior to and throughout the duration of the trial, the subjects were prohibited from ingesting any other medications, caffeine, grapefruit products, or alcoholic beverages. We requested that the patients stop taking medicines 2 days before the sample was obtained, and their doctors were satisfied with this from predose (0 hr), blood samples were obtained at nine time points until 24 hr post-dose (0, 0.5, 1, 2, 4, 6, 8, 12, 14 and 24). Storage conditions for the drug plasma samples were set at -20 °C until assayed. The following pharmacokinetic parameters of the preparations were calculated for each subject: C<sub>max</sub> (peak plasma concentration), t<sub>max</sub> (time to maximum plasma concentration), AUC (0-t) (the area under plasma concentration time curve 0 to 24 h), AUC (0-∞) (the area under plasma concentration time curve 0 to ∞), t<sub>1/2</sub> (elimination half-life), and K<sub>e</sub> (elimination rate constant) (Mano et al. 2011).

## 2.14. IVIVC correlation development

To develop IVIVC, data from the bioavailability study were used. The mean plasma concentration and mean release concentration of drug from SLM-M developed a graphical correlation. The predictive mathematical model describing an IVIVC is referred to as the correlation between an SLM-M *in vitro* property dosing method (usually the rate or extent of drug dissolution or release) (Kazi et al. 2018) and an appropriate *in vivo* reaction, such as plasma drug

concentration or dosage of the medication absorbed (Sankalia et al. 2008). Typically, a level of correlation is calculated by a two-step process that involves deconvolution and comparison of the fraction of drug dissolved to the fraction of drug absorbed. This kind of correlation shows a point-to-point relationship.

## 2.15. Hemolytic investigations

To conduct the hemolytic study, blood samples were collected in ethylene diamine tetra acetic acid tubes, which were centrifuged at 1500 rpm for 5 min, and the supernatant was removed. The resulting precipitate was washed 3 times with phosphatebuffer saline (PBS). A 200 µL volume of blood sediment was taken and washed, and 3.8 mL of phosphate buffer saline was added, followed by vortexing for a few minutes. These samples were kept at 37 °C for 2 h and then centrifuged for 5 min at 1600 rpm. Note the supernatant absorbance at 541 nm. In this experiment, purified water was selected as a positive control, and phosphate buffer saline was used as a negative control. The malformation of blood cells was observed through microscopy, and % hemolysis was determined by using the following equation (Assadi et al. 2018).

$$\% \text{Haemolysis} = \frac{\text{ABS} - \text{ABS0}}{\text{ABS100} - \text{ABS0}} \times 100$$

## 2.16. Acute toxicity studies

An animal model was used for SML-M per the toxicity guidelines of the Organization for Economic Co-operation & Development (OECD). Six rats weighing 150–170 g each were purchased from Tollinton market, Lahore, Pakistan. Animals were divided into two groups and kept in the animal house of Lahore University for fourteen days. The control group was provided access to food and water only, while the test group was orally administered SML-M along with water and food. On the 14th day of the study, blood samples were collected from both groups, and various biochemical parameters were examined (Erum et al. 2015; Badshah et al. 2021).

## 2.17. Drug content in the formulation (mini tablet)

Ten mini tablets were crushed and converted into fine powder. Accurately weighed 60.5 mg of fine powder was taken, and the contents were confirmed by using RP-HPLC at a wavelength of 250 nm. The results are summarized in Table 5.

## 2.18. wt. variation test of mini tablets

An electronic balance (Mettler-Toledo) was used to weigh ten mini tablets, and the test was performed according to the USP pharmacopeia (Chapter 2007).

## 2.19. Friability test of mini tablets

From each formulation, ten mini tablets were taken for the test. A range of maximum mean loss from three samples that should be not more than 1% is considered acceptable for most products (Chapter 2007). Table 5 shows the friability parameters of mini tablets.

## 2.20. Hardness of mini tablets

A Monsanto hardness tester was used to determine the hardness of 10 mini tablets (randomly). Hardness values were measured in kg/cm<sup>2</sup> (Chapter 2007). The mini tablet hardness results are shown in Table 5.



### 2.21. Accelerated stability study

The objective of the accelerated study was to determine the stability of drug moieties in microsponges (SML-M) in mini tablet form. A stability study of mini tablets was performed under forced degradation conditions (Patil et al. 2009). Mini tablets were placed in a stability chamber (Memmert HPP 1060 ECO). The temperature was set at  $45 \pm 1$  °C, and the relative humidity was kept at  $75 \% \pm 5$  for a period of 45 days (Usman et al. 2016). After 45 days, the mini tablets were crushed, and the drug contents of the mini tablets were determined by HPLC analysis.

## 3. Results

### 3.1. Percentage yield of solid dispersions

$\beta$ -Cyclodextrin- and NEOCEL C91-based sirolimus microsponges showed a yield of 90% for sirolimus: $\beta$ -cyclodextrin:NEOCEL C91 combination ratios of 47.5:47.5:5.5. The recorded yield was good enough, and there was no significant loss in the yield.

### 3.2. Drug content of solid dispersion

For all pharmaceutical preparations, fundamental quality attributes require a constant dose of drug between dispersions. The general limit for all solid dispersions to contain active ingredients is within 90–110%. The percent content of sirolimus in solid dispersion was satisfactory and was within the specification of 98.52%. Fig. 1.

### 3.3. Rheological studies of SLM-M

All the prepared SLM-M formulations were processed for rheological properties, and their results are shown in Table 2. It was found that raw material has low bulk density; on the other hand, solid dispersion bulk density was increased due to  $\beta$ -cyclodextrin and NEOCEL C91 in the formulation. The observed values for Carr's index, Hausner's ratio and angle of repose for SLM-M were 9.72%, 1.10 and 28.79°, respectively, which were in good agreement with those of the raw material. It was also evident that SMLM can be used for direct compression into mini tablets (see Table 3).

### 3.4. FT-IR spectroscopy

Fig. 2 displays the FTIR spectra of sirolimus,  $\beta$ -cyclodextrin, NEOCEL C91, and microsponges (SML-M). No noticeable peak

interference was visible in the FT-IR spectra of the various samples. Fig. 2 displays the sirolimus infrared spectrum. Fig. 2 shows the verified characteristic peaks of the functional groups that are present in the medication. Since functional sirolimus is fully characterized and identified by FTIR, it was used as a model drug for additional applications. The bands at  $3419 \text{ cm}^{-1}$  due to N-H stretching,  $2962 \text{ cm}^{-1}$  due to C = N stretching, and  $1726 \text{ cm}^{-1}$  due to carboxylate stretching could be seen in the FT-IR spectra of pure sirolimus. Additionally, the spectra revealed bands at  $1631 \text{ cm}^{-1}$  caused by C = O bending and at  $1107 \text{ cm}^{-1}$  caused by C-N bending. In the case of  $\beta$ -cyclodextrin, the bands at  $1023 \text{ cm}^{-1}$  and  $1080 \text{ cm}^{-1}$  are caused by the linked C-C and C-O stretching vibrations, while the band at  $1154 \text{ cm}^{-1}$  is caused by the antisymmetric stretching vibration of the C-O-C glycosidic bridge. Due to OH stretching vibration, which is also seen in SLM-M, the CD spectrum showed a strong peak at  $3423.99 \text{ cm}^{-1}$ . Fig. 2 depicts the infrared spectra of sirolimus solid dispersion with NEOCEL C91 and  $\beta$ -cyclodextrin. Chemical groups N-H stretching, C = N stretching, and carboxylate stretching were also observed in the spectrum; C = O bending and C-N bending with the same wavenumbers as sirolimus were also detected (Fig. 2).

Since sirolimus is primarily contained in  $\beta$ -cyclodextrin cavities, it cannot be clearly identified in the FT-IR spectra. The band associated with the stretching of sirolimus was superimposed, which caused the peak of the spectra in the area at approximately  $1080 \text{ cm}^{-1}$  to be widened and somewhat displaced. In the meantime, it was noted that the solid dispersion showed a shift of the sirolimus characteristic peak at  $1726\text{---}1728 \text{ cm}^{-1}$ .

### 3.5. Scanning electron microscopy (SEM)

Scanning electron microscopy (SEM) was used to determine the surface morphology and texture of the formulation. A round shape was observed, and the surface was free from drug crystals. The particle size of SLM-M (B) was 1–2  $\mu\text{m}$ , as shown in Fig. 3. The results showed that the SLM-M composite was not in crystal form but remained in the amorphous state in the microsponges (SLM-M).

### 3.6. Differential scanning calorimetry (DSC)

DSC was employed to examine the physical condition of SLM in pure form and inside the microsponges. Thermograms of the pure drug, polymers, and drug-loaded solid dispersion were obtained by scanning through a temperature range of 0–250 °C at a scanning rate of 10°/min. Fig. 4 displays the DSC spectra of a pure drug,  $\beta$ -cyclodextrin, NEOCEL C91 and microsponges (SLM-M). NEOCEL

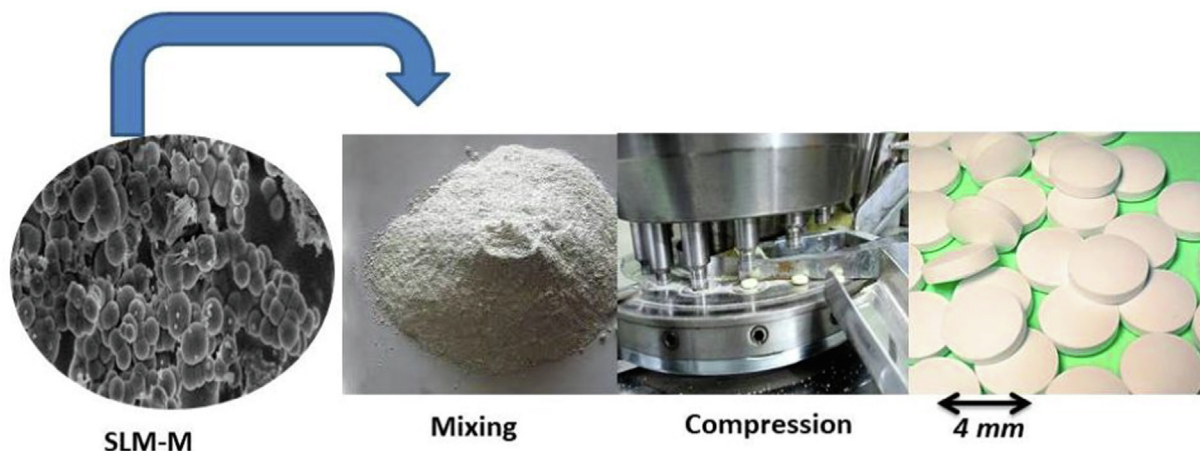


Fig. 1. Method of preparation of SLM-M compressed mini tablets (4 mm in diameter).

**Table 2**  
Rheological properties of Microsponges (SLM-M).

Formulation	Angle of Repose ( $\theta$ )	bulk density (gm/mL)	Tapped density (gm/mL)	Carr's index (%)	Hausner's ratio
SLM-M	28.79	0.678	0.751	9.72	1.10
SLM	34.15	0.620	0.799	22.40	1.29

**Table 3**  
Kinetic modeling of *in-vitro* dissolution data of SLM-M.

Formulation	pH	Zero Order Release Kinetics	First Order Release Kinetics	Higuchi Model	Korsmeyer–Peppas Model		Release Mechanism
		R <sup>2</sup>	R <sup>2</sup>	R <sup>2</sup>	R <sup>2</sup>	n	
SLM-M	1.2	0.985	0.964	0.963	0.955	0.891	Non Fickian diffusion
	7.4	0.994	0.893	0.992	0.984	0.634	Non Fickian diffusion

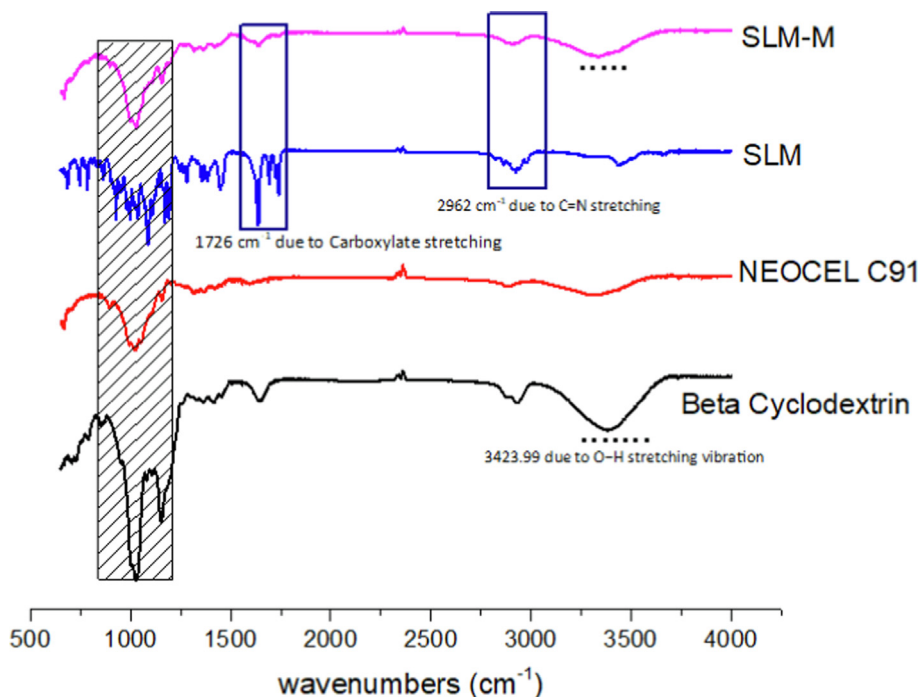


**Fig. 2.** FT-IR spectra of SLM, SLM-M, NEOCEL C91 and  $\beta$ -cyclodextrin.

C91 showed slight endothermic peak at 160 °C which was due to water molecules in NEOCEL C91. Endothermic peak was shown at 125.7 °C which is due to degradation of polymer.  $\beta$ -cyclodextrin polymers also showed endothermic peaks at which was started from 100 °C and end at 150.9 °C and it showed its thermal behavior. Pure sirolimus (SLM) showed acute endothermic melting peaks at nearly 30.08 °C which was due to water and one more endothermic peak at 181 °C.

In the heating scan, the SLM-M microsponges showed the same trend as neat drug at 180.3 °C. one of the peak observed at 154.43 which is due to polymers. In SLM-M we saw both polymers and drug peaks which shown its inclusion complex because drug peaks intensity was very low as compared to neat drug peak. Melting point of neat peak was slightly changed which may be due to inclusion complex. Some of the drug can be stick outside of the  $\beta$ -cyclodextrin cavity which shown extra peak in the SLM-M (183 °C).

**3.7. Powder X-ray diffraction (PXRD)**

PXRD examination was used to explore the crystalline and undefined state microsp sponge details of SD-SLM (Vo et al. 2013).

Fig. 5 displays the PXRD patterns of sirolimus,  $\beta$ -cyclodextrin, NEOCEL C91, and loaded solid dispersion. Sirolimus contains multiple peaks in its diffraction pattern, including those at 8.7°, 10.7°, 18.4°, 20.4°, and 27.6°. Sirolimus PXRD at 10.2, 15.4, 22.3, and 32.7 showed numerous broad and sharp peaks, demonstrating the highly crystalline structure of sirolimus. The NEOCEL C91 diffractogram and  $\beta$ -cyclodextrin both contained a few strong peaks, but their intensities were relatively modest. Additionally, some distinct peaks at 10.2, 15.4, 22.3, and 32.7 were discovered in SLM-M, confirming the inclusion of sirolimus in the formulation of the solid dispersion. However, additional peaks in SLM-M that were caused by  $\beta$ -cyclodextrin, NEOCEL C91, were also seen, but the data demonstrated that SLM-M crystallinity was decreased (Salonen et al. 2005).

**3.8. Drug release study**

Based on the cumulative release of sirolimus under different pH buffers, the release behavior of sirolimus from SLM-M is summarized in Fig. 6. The matching concentration values were determined using HPLC area measurements. The release behavior of sirolimus

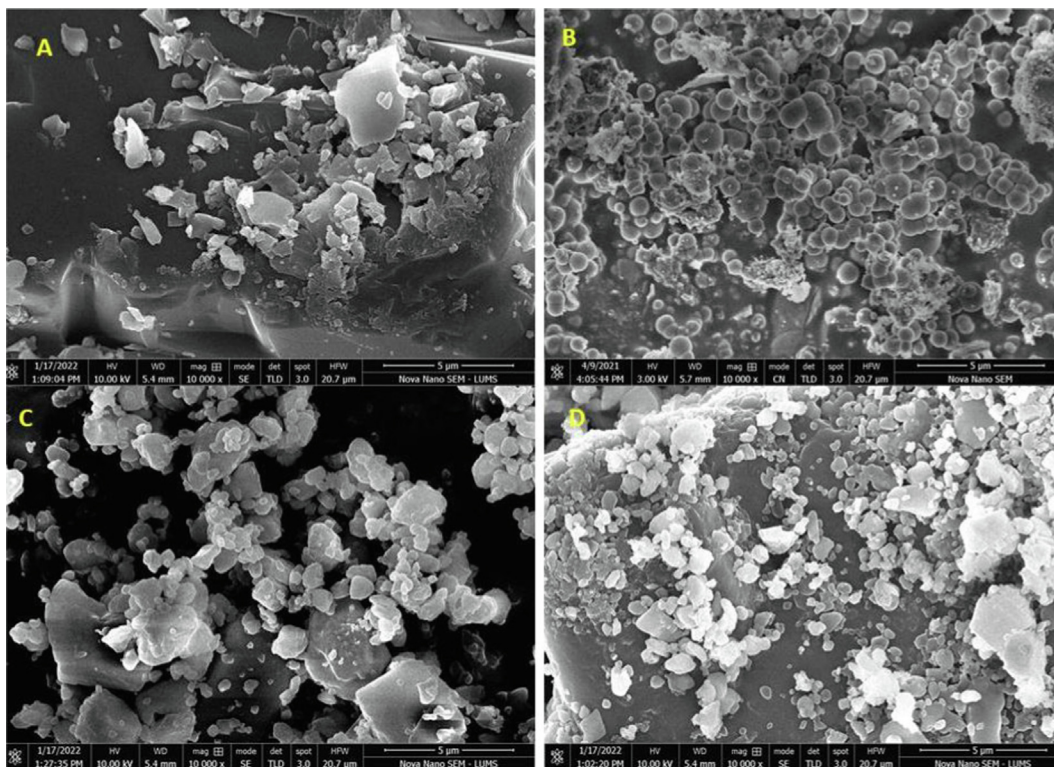


Fig. 3. Morphology of  $\beta$ -cyclodextrin (A), SML-M (B), NEOCEL C91 (C) and SLM (D).

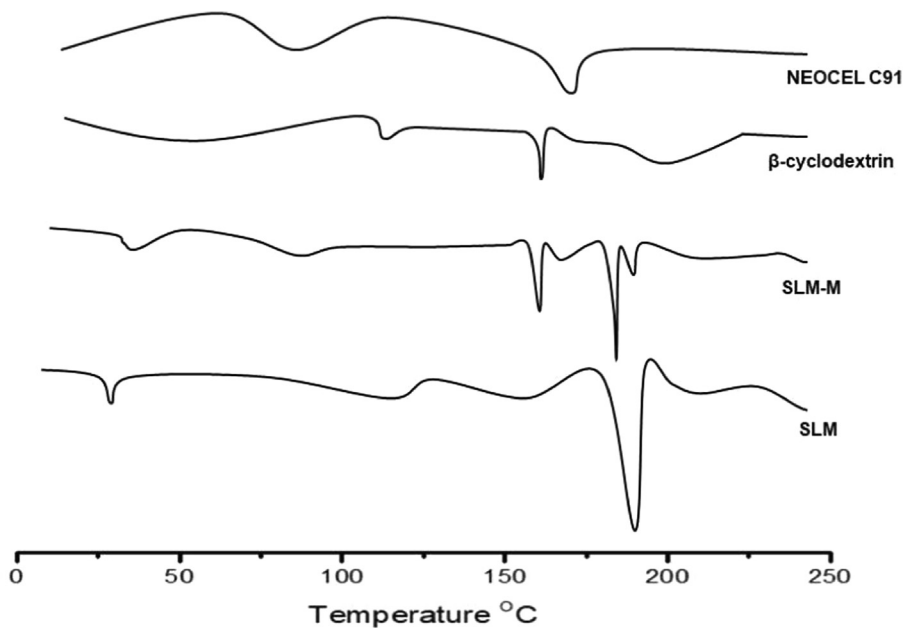


Fig. 4. DSC of NEOCEL C19,  $\beta$ -cyclodextrin, neat SLM and SLM-M.

(SLM) pure drug and SLM-M at pH 1.2 and pH 7.4 for 2 h was examined by a dissolution study, as shown in Fig. 6. It was found that SLM in pure form remained undissolved at both pH 1.2 and pH 7.4, whereas SLM-M showed more than 94 % of release at pH 1.2 in 60 min and 92 % release at pH 7.4 in 60 min. After 20 min, more than 75% of the drug was released in both pH buffers, and after 60 min, the release was complete.

### 3.9. Kinetic modeling for sirolimus

The correlation coefficient (R2) was used to estimate the drug release mode. Zero-order and first-order release models for SLM-M were found to have R2 values that ranged between 0.985 and 0.994 and 0.964 and 0.893 at both pH values, respectively. The regression coefficient (R2) values for SLM-M are tabulated in

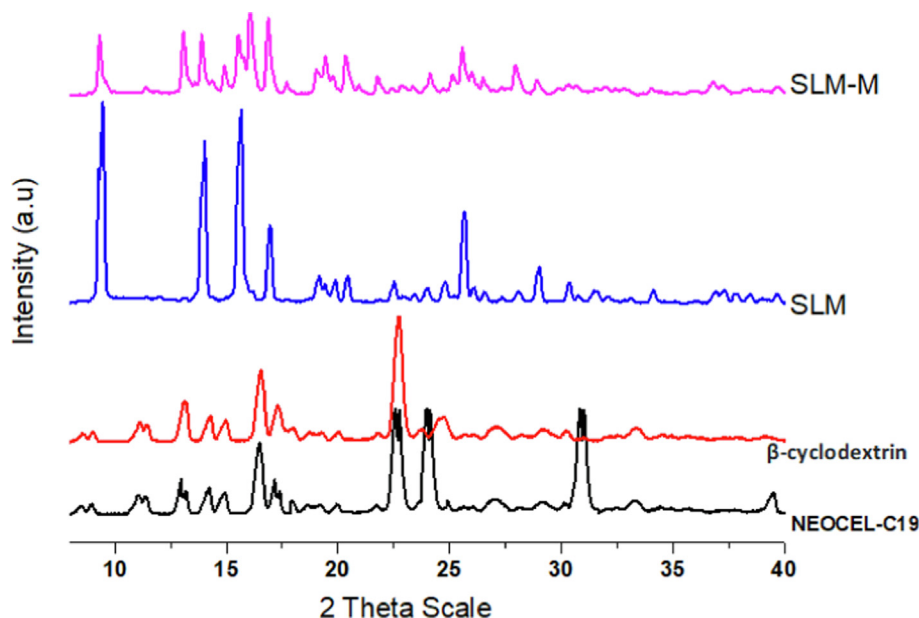


Fig. 5. XRD patterns of sirolimus,  $\beta$ -cyclodextrin, NEOCEL C91 and SML-M.

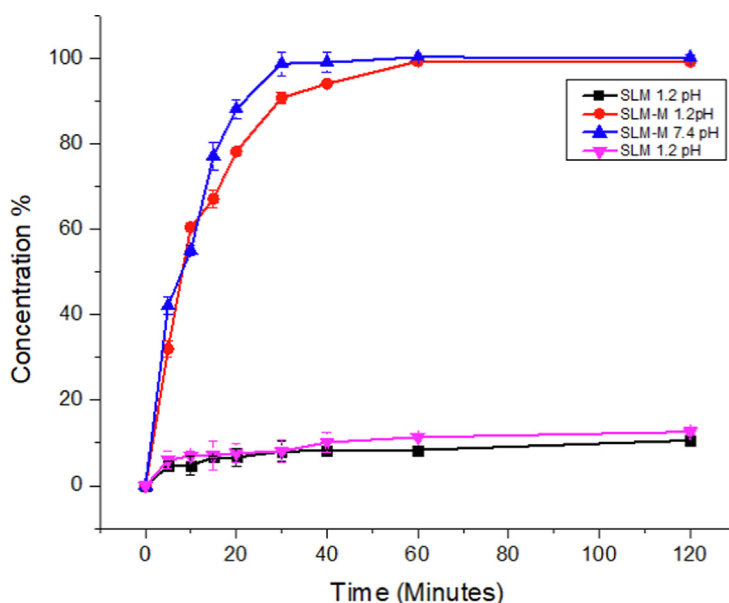


Fig. 6. Release profile of sirolimus from various formulations and raw drug at pH 1.2 and pH 7.4.

Table 2.  $R^2$  was higher in the zero-order release model, which showed that drug release is unrelated to concentration. Concerning drug release, the dosage forms following this profile, release the same amount of drug by unit time, and it is the ideal method of drug release in order to achieve a prolonged pharmacological action. In the case of micro sponge materials, one of the possibilities to incorporate non-constant diffusivity is the assumption that the diffusion coefficient of drugs depends on the matrix porosity. Following the non-Fickian method of drug transport, it was finally determined that both diffusion and erosion mechanisms were involved.

### 3.10. Cell viability

To study the cell viability effect of SLM-M against humans, a cell line (HepG2) was used. To measure the cell viability of SLM-M, an

MTT assay was performed. Different dilutions of SLM-M (50, 100, 200 and 1000  $\mu\text{g}/\text{mL}$ ) were exposed to the cell line for 24 h. After 24 h of incubation of SLM-M, 10  $\mu\text{L}$  of MTT reagent was incorporated into each well and incubated for 2 h. After incubation, a bioreader was used to read plates at 570 nm. The results indicated that SLM-M was safe and dose dependent. Cell viabilities at different concentrations are presented in Fig. 7.

### 3.11. In- vivo pharmacokinetics

Sirolimus prevents the formation of antibodies. In cells, sirolimus forms an immunosuppressive complex with immunophilin and FK Binding Protein-12 (FKBP-12). Following oral dosing in healthy people, hepatically compromised patients, and renal transplant patients, sirolimus pharmacokinetic activity data have been identified. In recipients of renal transplants, sirolimus is rapidly



absorbed, with a mean time to peak concentration (t<sub>max</sub>) of approximately two hours following a single dose. The SLM-M was delivered to humans to determine whether it enhanced the sirolimus solubility profile. Fig. 8 illustrates the blood concentration time profile of sirolimus after oral delivery of SLM-M at a dose of 1 mg/70 kg as sirolimus. Table 4 provides the neat sirolimus and SLM-M pharmacokinetic parameters. The blood levels of pure sirolimus (SLM) 0.5 mg in capsule were observed at low levels after oral administration of the crystalline powder, as shown in Fig. 8. In the case of neat sirolimus in capsule dosed at 0.51 mg/70 kg, the C<sub>max</sub> and AUC<sub>0-∞</sub> h values were 17.64 ng/mL and 170.44 ng h/mL, respectively (Table 4). However, when the SLM-M was given orally, the blood levels of sirolimus were significantly higher than crystalline SLM powder. The C<sub>max</sub> and AUC<sub>0-∞</sub> h of SLM-M were 31.84 ng/mL and 275.50 ng h/mL, respectively. The AUC and C<sub>max</sub> values for SLM-M were approximately two-fold higher than those for the crystalline SLM powder, indicating that higher oral absorption of sirolimus is possible due to the amorphous nature of the drug in SLM-M. These findings point to faster drug release from SLM-M solid dispersions, which led to higher bioavailability in humans. Due to the increased solubility of the drug in SLM-M compared to pure crystalline SLM, the drug was readily absorbed in the GI tract. These findings support the hypothesis that amorphous solid dispersion increases the solubility of sirolimus in GI fluids by maintaining the concentration gradient between lumen and blood, which results in enhanced permeability and bioavailability of the drug following oral administration (see Fig. 9).

### 3.12. IVIVC correlation development

An IVIVC can give the in vitro dissolution test in vivo context and serve as a stand-in for bioequivalence. To establish IVIVC, SLM-M underwent an in vivo investigation. Its results were compared with those of neat SLM for a number of pharmacokinetic parameters. Utilizing linear-nonlinear regression, a level A IVIVC for SLM-M was examined. IVIVC was used at 1.2 pH HCl dissolving media and pH 7.4 phosphate buffer at 50 rpm to explore the utilization of the percentage absorbed against % dissolved for the SLM-M formulation. With a regression coefficient of 0.9981 and a slope that is close to unity, a good point-to-point association was found, demonstrating a tight relationship between the in vitro release rates and their in vivo absorption.

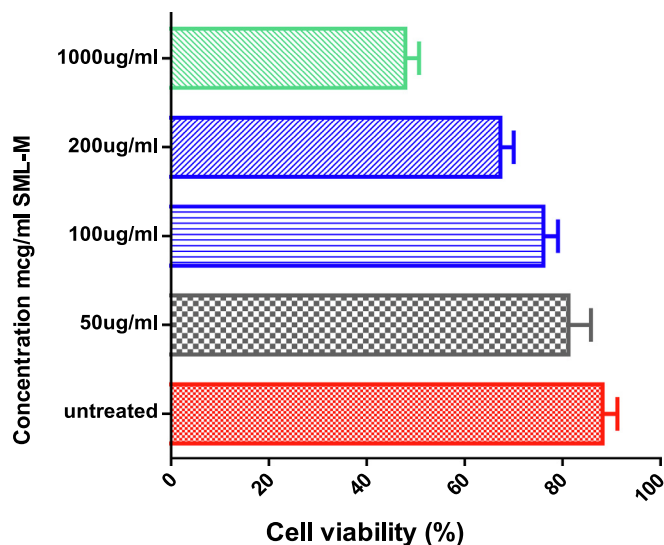


Fig. 7. Percentage viability induced at 50, 100, 200 and 1000 µg/ml SLM-M.

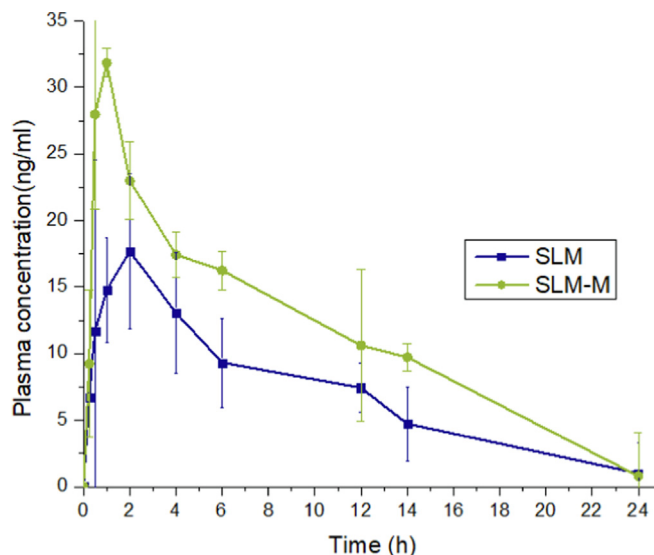


Fig. 8. Plasma concentration–time profile of pure sirolimus and in SLM-M after oral administration.

Table 4

Pharmacokinetic parameters of SLM and SLM-M after single-dose oral administration (0.5 mg) to humans.

Parameter	SLM	SLM-M
t <sub>1/2</sub> (h)	4.26 ± 0.155	3.20 ± 0.52
AUC <sub>0-∞</sub> (ng/mL*h)	170.44 ± 1.73	275.50 ± 4.49
T <sub>max</sub> (h)	2.0	1.0
C <sub>max</sub> (ng/mL)	17.64 ± 0.48	31.84 ± 0.054
λ <sub>z</sub> (1/h)	0.164 ± 0.001	0.221 ± 0.0041
MRT 0-inf_obs (h)	8.027 ± 0.12	7.68 ± 0.051

### 3.13. Internal validation

Convolution of the dissolution data that matched formulation using the IVIVC model served as the internal validation. In this pilot investigation, an internal predictability estimation for a level A IVIVC model for SLM-M formulation was produced. The absorption performance of SLM-M products with various release rates may be predicted using the IVIVC model, which may also be used to forecast the variance in site change, process change, scale-up, and absorption performance. The optimized SLM-M formulation was used to carry out internal validation while anticipating plasma awareness. Investigations were also made into the produced IVIVC’s predictability for the SLM-M. C<sub>max</sub> and AUC<sub>0-∞</sub> % PE both fell below 15% (Table 4). These outcomes demonstrated the developed IVIVC’s potential for application to in vivo performance prediction.

### 3.14. In vitro hemolytic activity

In vitro hemolytic activity studies were carried out by using a spectrophotometer. In this technique, clean human blood is collected in Eppendorf tubes. Special concentrations of SLM-M were organized in normal saline (50 µg/ml, 100 µg/ml, 200 µg/ml, and 400 µg/ml). Those concentrations were mixed with blood cells and incubated at 37°C for 24 h. As illustrated in Fig. 10, the hemolytic percentage was dose dependent. The maximum lysis activity of 400 µg/ml was 30% in SLM-M, suggesting that SLM-M is likely safe to use within 50–200 µg/ml.

**Table 5**  
Prediction errors (%) in  $C_{max}$  and  $AUC_{0-\infty}$  for Sirolimus IVIVC.

Formulation	$AUC_{0-\infty}$ (ng/mL*h)			$C_{max}$		
	Observed	Predicted	PE (%)	Observed	Predicted	PE (%)
SLM-M	12.50	10.99	12.08	32.84	28.93	11.91

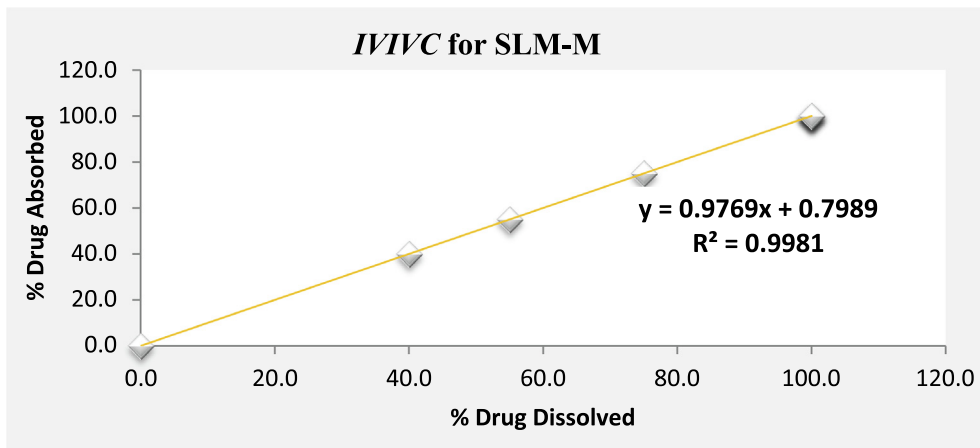


Fig. 9. Experimental and predicted in vivo release profiles of SLM-M.

### 3.15. Stability of drug in tablets

The stability of the drug in microspunge (SLM-M) mini tablets was determined by quantifying the degradants in the formulations. When subjected to exposure for 45 days at 45 °C/75% RH, the degradation was retarded in compressed mini tablets (approx. < 1%), and the results are shown in Table 6. Microspunge (SLM-M)-compressed mini tablets contained lactose and microcrystalline cellulose (MCC), which showed good physical and chemical stability with a lesser degree of degradation. In contrast, the market conventional SLM mini tablets showed 7% degradation under identical stability conditions, which is significantly higher than that recommended by the WHO guidelines. The cause for

API degradation under higher temperature and humidity conditions might be related to oxidation and hydrolysis (Javed et al. 2013; Yun et al. 2013).

### 3.16. Regulatory considerations

SLM, a white, triangular-shaped tablet with a 1-mg dose strength and a yellow to beige, triangular-shaped tablet with a 2-mg dose strength, are available commercially by the brand name Rapamune®. The major inactive ingredients include lactose, microcrystalline cellulose, and sucrose. SLM-M minitables meet all the innovator’s criteria for the reference drug per the regulatory requirements. The drug in oral tablet form also meets all USP 42 requirements. Therefore, drug manufacturers can readily adapt this innovative approach to scale up and produce this drug.

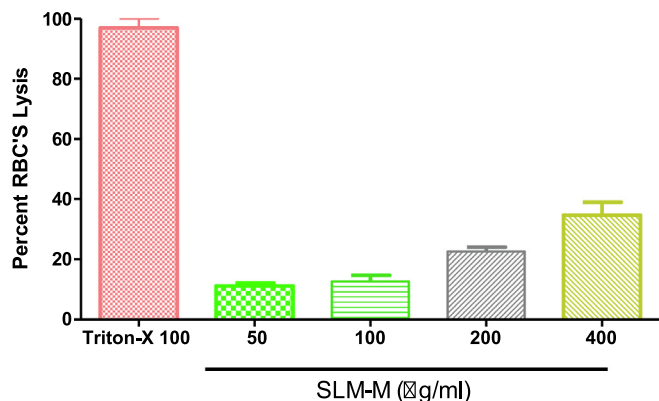


Fig. 10. Hemolytic activity of SLM-M against erythrocytes.

**Table 6**  
Drug content, weight variation, hardness and friability of mini tablets after compression and after accelerated study.

Code	Weight variation (%)	Hardness (kg/cm <sup>2</sup> )	Friability (%)	Drug content (%)
SLM-M Mini tablet	0.23	6.78	0.18	98.2
SLM-M Mini tablet 45 days	0.21	6.90	0.19	97.6

cyclodextrin and NEOCEL C91 loaded with sirolimus, which is an immunosuppressant drug. This combination is used for the first time in our research to enhance the bioavailability of immunosuppressant drugs. We used a  $\beta$ -cyclodextrin polymer with varying charges, solubility, and water permeability, which has strong binding properties with drugs. The successful design and fabrication of these adaptable microcarriers depends on the physicochemical characterization of microsponges. For the purpose of analyzing the structural and morphological characteristics of this delivery system, we used analytical methods such as Fourier transform infrared spectroscopy (FTIR), differential scanning calorimetry (DSC), powder X-ray diffraction (PXRD), scanning electron microscopy (SEM) and high-pressure liquid chromatography (HPLC). Based on these features, the functional aspects of microsponges were investigated. Moreover, we converted microsponges into mini tablets for patient use and compliance. Furthermore, a pharmacokinetic study and toxicity study of sirolimus microsponges were performed and found a significant increase in bioavailability and a decrease in toxicity. The stability of the drug in microsphere mini tablets was determined by quantifying the degradants in the formulations. When subjected to exposure for 45 days at 45 °C/75% RH, the degradation was retarded in compressed mini tablets (approx. < 1%). [Tiwari et al 2022](#) (Tiwari et al. 2022) have reported a range of methods for preparation of microsphere SLM minitables as drug delivery vehicles for different dosages, our method clearly demonstrates a significantly higher bioavailability. [Shen et al \(2018\)](#) (Shen et al. 2018) evaluated SLM nanoparticles in nanotables, prepared by anti-solvent method, and compressed with MCC, mannitol and HPMC with 2.5 mm in diameter, and examined the release profile and compared with marketed drug. The authors observed that dissolution in different simulated gastrointestinal pH was significantly higher than commercial tablets and reached 80% within 5 min at pH 6.8 in simulated intestinal pH of 6.8. With increasing the amount of HPMC to 15 wt%, the dissolution was similar to the marketed drug but was slower in the first 45 min with respect to marketed tablets. In contrast, in our case, the dissolution attained 100% release within 30 min with SLM microsphere minitables.

## 5. Conclusion

Sirolimus microsponges (SLM-M) were prepared by adapting a quasi emulsion-solvent diffusion technique. Microsphere technology is easily adaptable to improve the bioavailability of drugs. It has an excellent benefit by avoiding the use of organic solvents that may interfere with pharmacological responses and may pose long-term safety risks if not removed. In this study, we confirmed that the dissolution of sirolimus was improved significantly and was stable in microsponges designed with  $\beta$ -cyclodextrin. FTIR and DSC data showed no compelling impact on drug-polymer interactions that did not compromise the tablet performance in vitro and in vivo. SEM data showed the appropriate shape in surface morphology for drug entrapment. Microsponges of sirolimus showed good in vivo plasma exposure in humans, as was evident by the toxicology assessment of the molecule in rats. Taken collectively, this innovative approach of formulation has the potential to commercialize on a larger scale without any regulatory concerns.

## Institutional review board statement

The protocol was approved by the institutional review board of Rashid Latif College of Pharmacy and Medical College, guidelines of the Faculty of Pharmacy, Rashid Latif College of Pharmacy. Approval number: IRB No (RLCP/EP/13/2021).

## Funding

The project is funded by the Researchers Supporting Project Number (RSP2023R301), King Saud University, Riyadh, Saudi Arabia.

## Declaration of competing interest

The authors declare that they have no known competing financial interests or personal relationships that could have appeared to influence the work reported in this paper.

## Acknowledgments

The authors would like to extend their sincere appreciation to the Researchers Supporting Project Number (RSP2023R301), King Saud University, Riyadh, Saudi Arabia.

## References

- Aboulrous, A. A., T. Mahmoud, et al. 2016. Application of Natural Polymers in Engineering. Natural Polymers, Springer. 185-218.
- Aqil, M., A. A., Ahad, A., Sultana, Y., Najmi, A. K., Saha, N. 2007. "A validated hplc method for estimation of metoprolol in human plasma." ACTA CHROMATOGRAPHICA 19, 130-140.
- Badshah, S.F., Akhtar, N., et al., 2021. Porous and highly responsive cross-linked  $\beta$ -cyclodextrin based nanomatrices for improvement in drug dissolution and absorption. Life Sci. 267, 118931.
- Bansal, S.S., Goel, M., et al., 2011. Advanced drug delivery systems of curcumin for cancer chemoprevention. Cancer Prev. Res. 4 (8), 1158-1171.
- Beneke, C.E., Viljoen, A.M., et al., 2009. Polymeric plant-derived excipients in drug delivery. Molecules 14 (7), 2602-2620.
- Chapter, G. 2007. 1225, Validation of compendial methods, United States Pharmacopeia 30, National Formulary 25, Rockville, Md., USA, The United States Pharmacopeial Convention, Inc.
- Crini, G., 2005. Recent developments in polysaccharide-based materials used as adsorbents in wastewater treatment. Prog. Polym. Sci. 30 (1), 38-70.
- Deshmukh, A.S., Aminabhavi, T.M., 2015. Pharmaceutical applications of various natural gums natural gums. Polysaccharides: Bioactivity and Biotechnology, 1933-1967.
- Erum, A., Bashir, S., et al., 2015. Acute toxicity studies of a novel excipient arabinoxylan isolated from Ispaghula (Plantago ovata) husk. Drug Chem. Toxicol. 38 (3), 300-305.
- Haeri, A., Sadeghian, S., et al., 2017. Effective attenuation of vascular restenosis following local delivery of chitosan decorated sirolimus liposomes. Carbohydr. Polym. 157, 1461-1469.
- Huang, Y.-B., Tsai, Y.-H., et al., 2004. Once-daily propranolol extended-release tablet dosage form: formulation design and in vitro/in vivo investigation. Eur. J. Pharm. Biopharm. 58 (3), 607-614.
- Javed, I., Ranjha, N.M., et al., 2013. Accelerated stability studies of flurbiprofen film coated tablets of five different national brands in Pakistan. Journal of Drug Delivery and Therapeutics 3 (2).
- Kazi, M., Alanazi, F.K., et al., 2018. In vitro methods for in vitro-in vivo correlation (IVVC) for poorly water soluble drugs: lipid based formulation perspective. Curr. Drug Deliv. 15 (7), 918-929.
- Mano, N., Sato, M., et al., 2011. An accurate quantitative LC/ESI-MS/MS method for sirolimus in human whole blood. J. Chromatogr. B 879 (13-14), 987-992.
- Mohammadpour Dounighi, N., Mortazavi, S., et al., 2016. Preparation and in-vitro evaluation of sodium alginate microspheres containing diphtheria toxoid as new vaccine delivery. Arch. Razi Inst. 63 (2), 19-28.
- Montiel-Herrera, M., Gandini, A., et al., 2015. N-(furfural) chitosan hydrogels based on Diels-Alder cycloadditions and application as microspheres for controlled drug release. Carbohydr. Polym. 128, 220-227.
- Mosmann, T., 1983. Rapid colorimetric assay for cellular growth and survival: application to proliferation and cytotoxicity assays. J. Immunol. Methods 65 (1-2), 55-63.
- Mueller, R.H., Maeder, K., et al., 2000. Solid lipid nanoparticles (SLN) for controlled drug delivery—a review of the state of the art. Eur. J. Pharm. Biopharm. 50 (1), 161-177.
- Ormerod, A., Shah, S., et al., 2005. Treatment of psoriasis with topical sirolimus: preclinical development and a randomized, double-blind trial. Br. J. Dermatol. 152 (4), 758-764.
- Patel, S., Gheewala, N., et al., 2009. In-vitro cytotoxicity activity of Solanum nigrum extract against Hela cell line and Vero cell line. Int J Pharm Pharm Sci 1 (1), 38-46.
- Patil, K.R., Rane, V.P., et al., 2009. Stability-indicating LC method for analysis of lornoxicam in the dosage form. Chromatographia 69 (9-10), 1001-1005.
- Preetham, A., Satish, C., 2011. Formulation of a poorly water-soluble drug sirolimus in solid dispersions to improve dissolution. J. Dispers. Sci. Technol. 32 (6), 778-783.

- Rangan, G.K., Nguyen, T., et al., 2009. Therapeutic role of sirolimus in non-transplant kidney disease. *Pharmacol. Ther.* 123 (2), 187–206.
- Salonen, J., Laitinen, L., et al., 2005. Mesoporous silicon microparticles for oral drug delivery: loading and release of five model drugs. *J. Control. Release* 108 (2–3), 362–374.
- Sankalia, J.M., Sankalia, M.G., et al., 2008. Drug release and swelling kinetics of directly compressed glipizide sustained-release matrices: Establishment of level A IVIVC. *J. Control. Release* 129 (1), 49–58.
- Shazly, G., Mohsin, K., 2015. Dissolution improvement of solid self-emulsifying drug delivery systems of fenofibrate using an inorganic high surface adsorption material. *Acta Pharm.* 65 (1), 29–42.
- Shen, Y., Li, X., et al., 2018. Amorphous nanoparticulate formulation of sirolimus and its tablets. *Pharmaceutics* 10 (3), 155.
- Shen, L.-J., Wu, F.-L.-L., 2007. Nanomedicines in renal transplant rejection—focus on sirolimus. *Int. J. Nanomed.* 2 (1), 25.
- Tiwari, A., Tiwari, V., et al., 2022. Microsponges: a breakthrough tool in pharmaceutical research. *Future Journal of Pharmaceutical Sciences* 8 (1), 31.
- Usman, F., Javed, I., et al., 2016. Hydrophilic nanoparticles packed in oral tablets can improve the plasma profile of short half-life hydrophobic drugs. *RSC Adv.* 6 (97), 94896–94904.
- Vo, C.-L.-N., Park, C., et al., 2013. Current trends and future perspectives of solid dispersions containing poorly water-soluble drugs. *Eur. J. Pharm. Biopharm.* 85 (3), 799–813.
- Yun, Y., Cho, Y.W., et al., 2013. Nanoparticles for oral delivery: targeted nanoparticles with peptidic ligands for oral protein delivery. *Adv. Drug Deliv. Rev.* 65 (6), 822–832.
- Yuvaraja, K., Khanam, J., 2014. Enhancement of carvedilol solubility by solid dispersion technique using cyclodextrins, water soluble polymers and hydroxyl acid. *J. Pharm. Biomed. Anal.* 96, 10–20.
- Zaharuddin, N.D., Noordin, M.I., et al., 2014. The use of Hibiscus esculentus (Okra) gum in sustaining the release of propranolol hydrochloride in a solid oral dosage form. *Biomed Res. Int.*